Biosynthesis of Ganefromycin: Results from Blocked Mutants and Bioconversion Experiments

Leonard A. McDonald, Jason A. Lotvin, Arthur E. Bailey, and Guy T. Carter*

Departments of Natural Products Chemistry and Bioprocess Development, Wyeth-Ayerst Research, North Middletown Road, Pearl River, New York 10965

Received September 3, 1997

The biosynthetic pathway of ganefromycin α (**8**) was investigated using blocked mutants of *Streptomyces lydicus* spp. *tanzanius*, the ganefromycin α producer, in conjunction with bioconversion experiments with the products of these mutants. Compounds **1**−**7** and **9**−**15**, which are structurally related to ganefromycin α, were produced by cultures of secretor mutants showing blockage or diminished production of **8**. These compounds were isolated, characterized, and subjected to bioconversion experiments using converter and other secretor mutants. Some of the compounds were shown to be products resulting from blocks at various stages in the biosynthetic pathway beyond construction of the polyketide skeleton (e.g., furan ring closure, hydroxylation, glycosylation, etc.). Other compounds were not bioconverted by biosynthetically capable mutants and were deemed shunt products. A mutant's metabolites and bioconverting ability were used to surmise the location of the block. A picture of the later sequence of events leading to the synthesis of ganefromycin α emerged, including C23-hydroxylation, C13a-*O*-methylation, C21a-hydroxylation, and C21a-*O*-glycosylation. Some of the later steps in the biosynthetic pathway for ganefromycin α are proposed.

Ganefromycins, a family of elfamycin antibiotics produced by S*treptomyces lydicus* spp. *tanzanius* Lechevalier (Streptomycetaceae), have shown excellent growth-promoting activity in animals.[1,2] A series of ganefromycin antibiotics (**1**−**7** and **9**−**15**) has been isolated and identified in order to establish their biosynthetic relationships to the previously reported ganefromycin α (**8**). The biogenesis of the aglycon of **8** and other elfamycin antibiotics is clearly polyketide. Preliminary investigations suggested that the aglycon of **8** arises from the joining of two polyketides, one derived from a propionate and five acetate units and the other stemming from an undetermined starter unit and seven or eight acetate units. The four *O*-methyl and four *C*-methyl groups of **8** were shown to originate from methionine.[3] Later studies demonstrated that the methylation inhibitor sinefungin inhibited the production of **8** and caused accumulation of des-*O*-methyl intermediates,[4] suggesting that *O*-methylation is crucial for complete biosynthesis of **8**. The origin of the phenacyl and the trisaccharide units has not been established, and the sequence of elaboration of the ganefromycin aglycon to the ultimate antibiotic also remained unknown.

Reports of biosynthetic studies on the related compound aurodox suggested that the molecule was composed of a polyketide fragment derived from one butyrate and five acetate units joined via an amide bond to another fragment originating from one propionate and eight acetate units.[5,6] A subsequent report on the biosynthesis of efrotomycin, a disaccharide of aurodox, apparently confirmed the biosynthetic origin of the backbone and suggested that the amide nitrogen and the two adjacent carbon atoms were derived from glycine.[7]

Many metabolites structurally related to ganefromycin α (**8**) were found in cultures of the wild-type antibiotic-producing strain.[8,9] Some of these compounds were thought likely intermediates in the biosynthesis of **8**.[10] Intermediates or their shunt products, normally present in low steady-state concentrations in the wild-type strain, can accumulate in genetically defective mutants blocked in the production of the antibiotic. Analogues that may be inaccessible by chemical synthesis could be obtained in this manner and could afford valuable structure−activity information. The intermediates, if shown to be direct precursors of the antibiotic, could also provide valuable biosynthetic information. The present study seeks to establish some of the later biosynthetic events in the pathway to **8** by generating blocked mutants from *S. lydicus* spp. *tanzanius* and carrying out bioconversion experiments with the metabolites from the mutants. The location of the block in the mutants, accumulated metabolites, and bioconversion of isolated intermediates allowed the elucidation of several of the later steps in the biosynthetic pathway to ganefromycin α.

Results and Discussion

Isolation and Characterization of Mutants. Ganefromycin α-producing strain LL2057, a high-level producer of **8** derived from *S. lydicus* spp. *tanzanius* NRRL 18036, was chosen as the starting point for isolation of blocked mutants. Colonies derived from *N*-methyl-*N*′-nitro-*N*-nitrosoguanidine (NTG)[11] treated cells were tested for antibiotic production by overlaying with *Bacillus megaterium*, an organism exquisitely sensitive

* To whom correspondence should be addressed. Phone: (914) 732-3594. Fax: (914) 732-5536. E-mail: carterg@war.wyeth.com.

S0163-3864(97)00408-4 CCC: $15.00
Published on Web 02/10/1998

Scheme 1. Structures of Elfamycin Antibiotics **1**−**15**

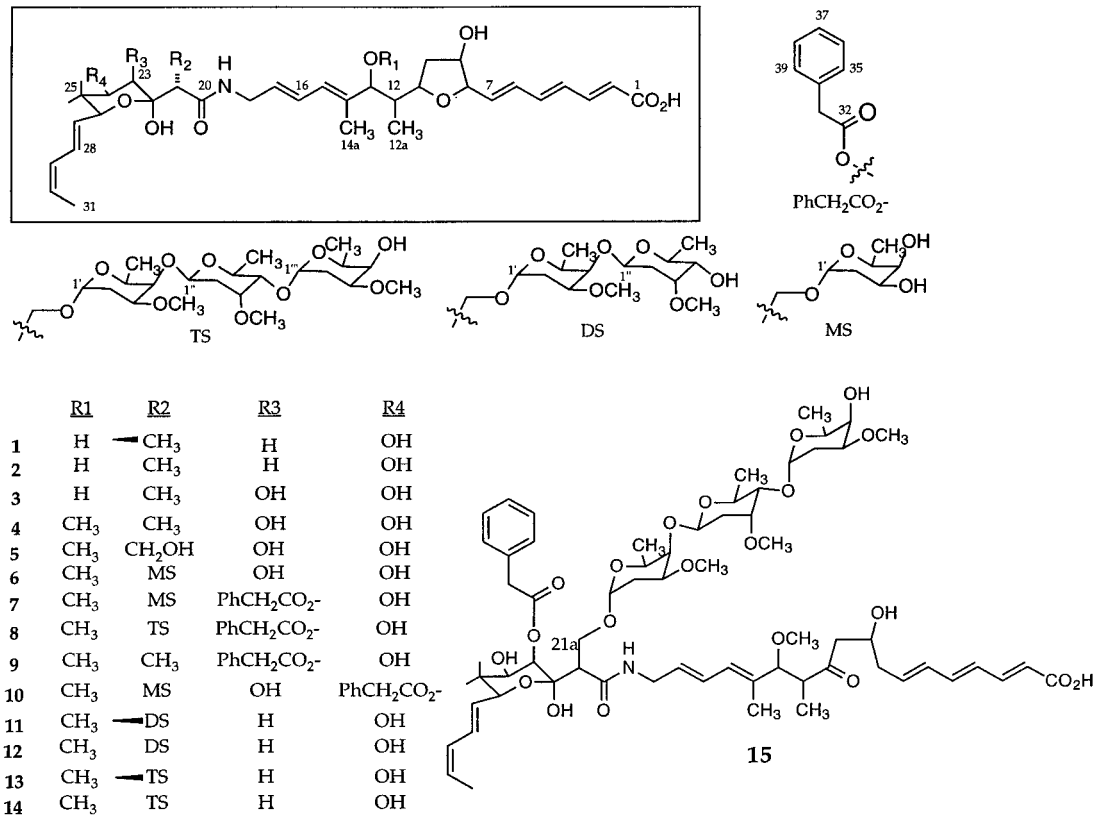

	R1	R2	R3	R4
1	H	CH_3	H	OH
2	H	CH_3	H	OH
3	H	CH_3	OH	OH
4	CH_3	CH_3	OH	OH
5	CH_3	CH_2OH	OH	OH
6	CH_3	MS	OH	OH
7	CH_3	MS	$PhCH_2CO_2$-	OH
8	CH_3	TS	$PhCH_2CO_2$-	OH
9	CH_3	CH_3	$PhCH_2CO_2$-	OH
10	CH_3	MS	OH	$PhCH_2CO_2$-
11	CH_3	DS	H	OH
12	CH_3	DS	H	OH
13	CH_3	TS	H	OH
14	CH_3	TS	H	OH

to **8**. Colonies showing no inhibition of the test organism were recovered and tested to reconfirm the block. Thirty-two mutants were identified that showed either no agar bioactivity or significantly reduced activity and minimal to no antibiotic production in liquid fermentations analyzed by HPLC. These mutants were preliminarily classified as converters, secretors, or noncomplementors based on agar cosynthesis (directional cross-feeding). Once classified, secretor and representative converter mutants were analyzed more thoroughly by HPLC for accumulated products and bioconversion ability.

Cosynthesis. Mutants were analyzed for directional cross-feeding on agar. Four main classes emerged. Class I mutants converted intermediates secreted from Class II and III mutants to bioactive product. The vast majority of mutants (25 of 32) were classified as such. Mutant B3M18 exemplified this class; it showed no evidence of bioactivity on agar and showed no ganefromycin-like peaks by HPLC analysis. A unique member of this class, LL2238, showed no bioactivity on agar and converter behavior identical with B3M18, but did show a ganefromycin-related metabolite by HPLC−UV, which was ultimately identified as **15**.

Mutant B3M39 is the only member of Class II. It was identified as secreting intermediates that were converted to a weakly bioactive product by Class I mutants.

Class III mutants secreted intermediates that were converted to a strongly active product by Class I mutants on agar. Mutants LL2241 (and the identical mutants LL2240 and LL2243), LL2239, and LL4208 were placed in this class.

Mutant LL2237 is the only representative of Class IV. No observable intermediates were accumulated, and mutant LL2237 showed no complementation interactions with any other blocked mutant. This mutant is presumed to contain either a regulatory mutation or a pathway deletion. No biosynthetic work was done (or was feasible) with this class.

Accumulation, Isolation, and Characterization of Ganefromycin Intermediates. Fermentation samples (~5 mL) of each mutant were analyzed by HPLC to examine the metabolite profile. Compounds were visualized by diode-array UV detection and characterized as ganefromycin-type intermediates based on their UV spectra. New compounds ultimately isolated from larger scale (0.3 to 3 L) fermentations served as reference standards, allowing identification of most compounds observed during bioconversion studies.

Compounds **1**−**7** and **9**−**15** were isolated from mutants of *S. lydicus* blocked in the biosynthesis of ganefromycin α (**8**). Isolation was accomplished by solid-phase HP20 resin extraction of the metabolites from the cultured broth followed by stepwise desorption of the compounds from the resin to afford partial refinement and finally purification by reversed-phase HPLC. The structures of the compounds were established as shown in Scheme 1 by examination of NMR spectroscopic and mass spectrometric data and by comparison with the data for **8**.[8]

Although easily separable by HPLC, compounds **1** and **2** had the same molecular weight and appeared to be identical by NMR except for atoms proximal to C21 (Tables 1 and 2). During structure elucidation, proton resonances corresponding to **2** were readily apparent in a deuteriomethanol solution of **1** after 34 days. The H-21 proton resonance in the mixture was diminished relative to the others, consistent with deuterium ex-

Table 1. ^{1}H-NMR[a] Assignments for Elfamycin Antibiotics **1**−**7**, **9**−**12**, **14**, and **15**

atom no.	**1**[b]	**2**[b]	**3**[b]	**4**[b]	**5**[b]	**6**[c]	**7**[c]	**9**[d]	**10**[c]	**11**[c]	**12**[c]	**14**[c]	**15**[d]
2	5.90	5.89	5.89	5.89	5.89	5.91	5.93	5.85	5.92	5.91	5.93	5.92	5.85
3	7.30	7.31	7.30	7.31	7.29	7.32	7.33	7.28	7.32	7.31	7.31	7.31	7.36
4	6.44	6.44	6.44	6.44	6.44	6.44	6.44	6.31	6.43	6.43	6.43	6.43	6.26
5	6.67	6.68	6.68	6.69	6.69	6.72	6.73	6.59	6.73	6.73	6.73	6.72	6.56
6	6.42	6.42	6.42	6.42	6.42	6.44	6.43	6.44	6.43	6.43	6.43	6.43	6.24
7	6.05	6.05	6.04	6.05	6.05	6.10	6.12	6.00	6.11	6.10	6.10	6.10	5.98
8	4.37	4.37	4.37	4.34	4.34	4.37	4.37	4.40	4.37	4.37	4.37	4.37	2.36
9	4.30	4.31	4.31	4.29	4.28	4.35	4.35	4.37	4.35	4.35	4.35	4.35	4.23
10	2.03	2.04	2.03	2.03	1.98	1.97	1.98	1.97	1.97	1.97	1.97	1.96	2.77
													2.58
11	4.68	4.68	4.68	4.65	4.65	4.61	4.63	4.67	4.61	4.62	4.61	4.63	
12	1.73	1.73	1.73	1.74	1.74	1.62	1.67	1.72	1.66	1.66	1.67	1.67	2.84
12a	0.74	0.74	0.74	0.71	0.71	0.70	0.73	0.74	0.72	0.71	0.72	0.72	0.82
13	3.92	3.92	3.92	3.87	3.85	3.38	3.41	3.43	3.39	3.39	3.39	3.39	3.62
13a				3.15	3.15	3.13	3.14	3.18	3.13	3.14	3.13	3.14	3.07
14a	1.72	1.72	1.72	1.63	1.63	1.65	1.65	1.65	1.64	1.64	1.64	1.64	1.67
15	5.99	5.98	5.98	5.98	5.98	5.97	5.99	5.96	5.98	5.99	5.99	5.99	5.99
16	6.47	6.46	6.47	6.47	6.47	6.49	6.51	6.39	6.52	6.49	6.54	6.53	6.41
17	5.66	5.63	5.62	5.63	5.63	5.66	5.65	5.61	5.67	5.66	5.69	5.68	5.63
18	3.86	3.85	3.85	3.87	3.91	3.92	3.93	3.87	3.86	3.94	3.93	3.91	3.91
						4.01	4.01		4.01	3.99	4.01	4.01	
19						7.76	7.61	5.37	7.78	7.31	7.68	7.68	5.57
21	2.55	2.54	2.97	2.97	3.11	3.20	2.95	1.83	3.23	2.76	2.82	2.82	2.32
21a	1.19	1.21	1.21	1.22	3.90	3.66	3.38	0.88	3.60	3.79	3.61	3.62	3.74
						3.89	3.80		3.87	3.97	3.90	3.90	
23	1.72	1.44	3.66	3.66	3.85	4.08	5.01	5.02	3.80	1.67	1.47	1.47	4.94
	1.97	1.91								1.94	1.85	1.85	
24	3.72	3.73	3.59	3.60	3.60	3.58	3.82	3.90	4.95	3.73	3.74	3.72	3.89
25a	0.72	0.76	0.91	0.91	0.91	0.92	0.89	0.87	1.01	0.75	0.76	0.76	0.86
25b	0.89	0.92	0.90	0.90	0.91	0.91	0.93	0.92	0.69	0.91	0.93	0.93	0.91
26	4.15	4.16	4.23	4.23	4.22	4.22	4.31	4.26	4.33	4.18	4.17	4.17	4.28
27	5.62	5.63	5.62	5.63	5.63	5.66	5.68	5.55	5.64	5.62	5.66	5.67	5.58
28	6.55	6.52	6.54	6.54	6.54	6.59	6.58	6.42	6.61	6.56	6.58	6.58	6.46
29	6.00	6.00	6.00	6.00	6.00	6.01	6.03	5.99	6.01	6.01	6.01	6.01	5.98
30	5.47	5.47	5.47	5.47	5.48	5.46	5.50	5.50	5.47	5.46	5.47	5.47	5.52
31	1.73	1.73	1.73	1.73	1.74	1.73	1.75	1.74	1.75	1.75	1.75	1.73	1.76
33							3.71	3.67	3.72				3.66
35							7.33	7.33	7.34				7.31
36							7.32	7.29	7.31				7.31
37							7.27	7.29	7.27				7.25
38							7.32	7.29	7.31				7.31
39							7.33	7.33	7.34				7.31
1′						4.80	4.66		4.78	4.83	4.86	4.86	4.64
2′						1.66	1.71		1.66	1.59	1.59	1.60	1.65
						1.78	1.81		1.80	1.84	1.84	1.86	1.97
3′						3.87	3.85		3.50	3.48	3.48	3.36	
3′a										3.32	3.33	3.32	3.37
4′						3.50	3.49		3.51	3.91	3.92	3.91	3.77
5′						3.78	3.71		3.76	3.74	3.73	3.75	3.59
6′						1.16	1.16		1.16	1.17	1.17	1.17	1.18
1″										4.75	4.75	4.80	4.70
2″										1.52	1.52	1.53	1.72
										2.29	2.30	2.31	2.38
3″										3.60	3.61	3.75	3.74
3″a										3.42	3.42	3.42	3.39
4″										3.14	3.12	3.21	3.30
5″										3.61	3.61	3.83	3.81
6″										1.18	1.19	1.18	1.25
1‴												4.95	4.99
2‴												1.79	1.90
												1.86	
3‴												3.54	3.67
3‴a												3.31	3.36
4‴												3.76	3.79
5‴												4.03	4.01
6‴												1.21	1.31

[a] Proton data acquired at 300 MHz. [b] Assignments made in CD_3OD. [c] Assignments made in MeCO-d_6. [d] Assignments made in $CDCl_3$.

change previously proposed.[9] After 62 days in solution, HPLC showed that **1** had epimerized to an approximately 50:50 mixture of **1** and **2**. Under identical solution conditions, compound **2** appeared to be stable and remained unchanged. A ROESY experiment carried out on a freshly isolated sample of **1** showed correlations between H-21a and both H-23ax (strong) and H-23eq (medium). H-23eq also showed a weak correlation to H-21, supporting the structure shown in Figure 1. A similar ROESY experiment run on **2** also showed correlations between H-21a and both H-23ax (medium) and H-23eq (strong); however, the intensities

Table 2. ^{13}C-NMR[a] Assignments for Elfamycin Antibiotics **1**−**7**, **9**−**12**, **14**, and **15**

atom no.	**1**[b]	**2**[b]	**3**[b]	**4**[b]	**5**[b]	**6**[c]	**7**[c]	**9**[d]	**10**[c]	**11**[c]	**12**[c]	**14**[c]	**15**[d]
1	170.74	170.46	170.62	170.51	NOe	167.71	167.69	N.O.[e]	167.60	167.71	167.71	167.67	170.83
2	122.76	122.24	122.51	122.29	123.22	121.69	121.61	121.73[f]	122.32	121.74	121.75	121.87	119.76
3	145.99	146.24	146.09	146.21	145.63	145.56	145.49	145.49	145.52	145.53	145.52	145.46	146.39
4	131.25	131.13	131.18	131.14	131.34	130.50	130.35[†]	130.30	130.55	130.29[‡]	130.29[‡]	130.30[‡]	128.52
5	141.32	141.51	141.40	141.49	141.11	141.28	141.21	140.06	141.25	141.27	141.26	141.23	141.32
6	132.95	132.87	132.90	132.94	133.05	131.52	131.53	132.22	131.53	131.50	131.50	131.42	132.39
7	136.02	136.17	136.10	136.27	136.68	137.61	137.53	134.19	137.59	137.61	137.61	137.60	135.73
8	85.13	85.08	85.10	85.07	85.13	84.29	84.30	83.28	84.30	84.29	84.30	84.23	39.74
9	75.36	75.34	75.36	75.57	75.59	75.06	75.05	74.68	75.06	75.05[§]	75.16[§]	75.04[§]	66.99
10	39.75	39.74	39.75	40.14	40.13	40.32	40.28	39.23	40.32	40.35	40.36	40.26	50.13
11	79.18	79.10	79.09	77.66	77.45	78.19	78.15	77.75	78.19	78.22	78.22	78.07	214.44
12	41.35	41.23	41.25	40.99	41.00	40.66	40.62	39.89	40.66	40.70	40.66	40.59	48.01
12a	10.93	10.89	10.88	10.44	10.42	10.63	10.60	10.12	10.63	10.66	10.67	10.59	13.34
13	80.95	80.91	80.93	90.84	90.89	90.26	90.23	89.26	90.25	90.35	90.33	90.30	89.89
13a				56.31	56.30	56.21	56.21	56.05	56.21	56.17	56.17	56.18	56.03
14	140.14	140.10	140.03	136.82	136.68	137.00	137.23	136.80	137.02	136.86	137.08	137.08	134.61
14a	11.61	11.57	11.54	10.96	10.96	11.05	11.05	10.82	11.04	11.09	11.06	11.04	10.67
15	127.66	127.60	127.66	127.93	130.35	129.66	129.56	128.43	129.65	129.66	129.56	129.54	129.53
16	129.00	128.78	128.73	128.23	128.13	128.11	128.38	128.54	128.14	127.91	128.13	128.14	127.88
17	130.19	129.87	129.97	130.47	130.61	130.61	130.32	128.35	130.30	130.64	130.62[¥]	130.59[¥]	129.53
18	42.34	42.06	42.05	42.00	42.17	41.84	41.88	41.28	41.84	41.86	42.01	41.87	41.53
20	175.58	177.98	179.09	179.12	176.38	175.40	174.90	175.95	175.33	172.41	174.86	174.85	173.36
21	52.65	50.05	44.50	44.54	42.17	50.20	49.84	43.62	49.74	57.74	55.10	55.03	49.79
21a	12.41	13.45	13.25	13.23	60.85	64.96	64.13	12.61	64.70	65.89	65.06	64.97	63.48
22	99.19	99.64	101.18	101.18	100.15	99.40	98.51	98.69	99.60	98.07	98.15	98.15	97.27
23	35.58	37.93	71.09	71.10	71.99	68.03	72.60	71.34	69.18	38.08	39.52	39.47	71.95
24	72.95	72.60	73.93	73.93	73.81	72.88	72.07	72.44	76.58	71.70	71.54	71.46	72.25
25	40.33	40.22	39.83	39.83	39.96	39.54	39.62	38.71	38.82	39.92	39.99	39.99	38.78
25a	12.41	12.40	15.83	15.84	15.77	15.79	15.37	14.78	16.81	12.39	12.42	12.42	14.72
25b	23.04	23.05	24.63	24.64	24.55	24.38	24.26	23.71	24.01	23.00	23.00	22.99	23.69
26	78.64	77.91	77.64	77.66	78.89	76.39	76.85	76.65	76.44	77.74	76.74	76.72	76.40
27	130.24	130.27[†]	130.40	130.41	130.57	130.59[†]	130.02[‡]	128.14	129.73	130.97	130.65[¥]	130.63[¥]	128.13
28	128.63	128.18	127.92	127.93	127.97	127.07	127.51	127.58	127.64[†]	127.64	127.23	127.20	127.56
29	130.36	130.29	130.43	130.44	130.44	130.29	130.18[‡]	129.08	130.15	130.31[‡]	130.32[‡]	130.26[‡]	129.01
30	126.91	126.70	126.56	126.55	126.64	125.94	126.35	126.21	126.42	126.23	125.98	125.97	126.29
31	13.56	13.63	13.62	13.62	13.64	13.57	13.58	13.44	13.57	13.54	13.57	13.56	13.44
32							171.50	171.45	171.38				171.45
33							41.72	41.95	41.78				41.73
34							135.41	134.17	135.70				133.90
35							130.36	129.68	130.28				129.53
36							129.17	128.63	129.16				128.63
37							127.61	127.16	127.67				127.12
38							129.17	128.63	129.16				128.63
39							130.36	129.68	130.28				129.53
1′						97.81	97.35		97.73	99.12	97.59	97.57	97.00
2′						33.39	33.25		33.38	32.17	32.16	32.13	31.02
3′						66.08	66.07		66.06	75.12[§]	75.17[§]	75.16	74.37
3′a										55.38	55.47	55.48	55.57
4′						71.64	71.60		71.63	74.12	74.23	74.34	74.22
5′						66.89	66.88		66.90	67.44	67.39	67.36[∞]	66.44
6′						17.28	17.17		17.27	17.83	17.80	17.79	17.15
1″										99.55	99.56	99.41	98.99
2″										34.83	34.84	34.66	32.94
3″										8.82	78.84	77.82	77.20
3″a										57.75	57.75	57.21	56.49
4″										73.90	73.92	82.73	81.66
5″										71.28	71.29	69.65	69.11
6″										18.62	18.66	18.61	18.07
1‴												101.13	100.57
2‴												30.92	29.89
3‴												75.73	74.37
3‴a												55.19	55.42
4‴												67.79	67.54
5‴												67.33[∞]	66.02
6‴												17.46	16.95

[a] Carbon data acquired at 75 MHz. [b] Assignments made in CD_3OD. [c] Assignments made in MeCO-d_6. [d] Assignments made in $CDCl_3$. [e] Resonance not observed. [f] Not observed in the ^{13}C or DEPT spectrum but observed as a cross-peak in the HMQC spectrum. [†,‡,§,¥,∞]Assignments with the same symbol within columns are interchangeable.

of these correlations were reversed, and an additional strong correlation between H-23ax and H-21 supports the structure for **2** shown in Figure 1. The difference between **1** and **2** appears to be the stereochemistry at C21.

Identical molecular weights for **11** and **12**, in addition to virtually identical spectral characteristics, suggested a relationship between this pair similar to that between **1** and **2**. The most dramatic spectral differences between compounds **11** and **12** were the chemical shifts

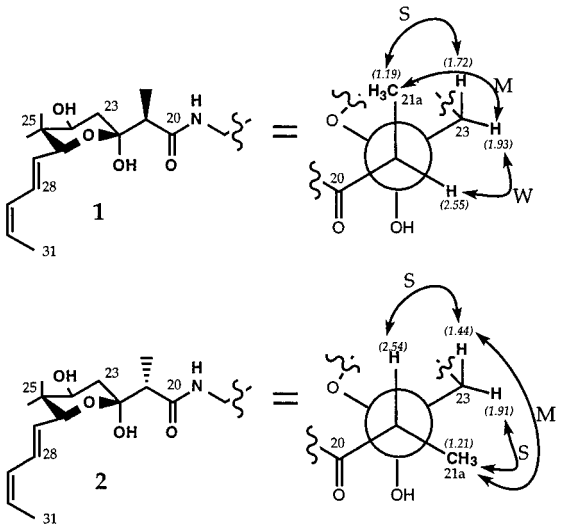

Figure 1. Significant ROESY correlations for 1 and 2. S = strong, M = medium, and W = weak.

of carbons 18, 20, 21, and 21a. Conversion of **11** to **12** began to occur in the fractions containing **11** eluting from the preparative HPLC column. This resulted in the structures of **11** and **12** being determined simultaneously using a deuterioacetone solution that was initially predominantly **11** but ultimately converted to a 50:50 mixture of **11** and **12** at the end of the NMR experiment. Isolated **12** was stable under identical NMR experimental conditions and was used for structure confirmation. Compounds **13** and **14** share the same relationship as **1** and **2**. Compound **13** was converted entirely to **14** during workup of fractions from the HPLC and could not be characterized by NMR.

The trend that emerged for these C21 epimeric pairs is that the epimer with the same C21 stereochemistry as **1** (**11** and **13**) were less stable and readily converted to form the other epimer. The larger substituent on the C21a position is more destabilizing to the "unstable" epimer. These less stable epimers also elute first from a C18 HPLC column (Table 3).

Biological Activity of Ganefromycin Metabolites. MIC values against *B. megaterium* were determined for all isolated compounds by the tube dilution method (Table 4). The parent compound **8** is the most active, while the nonglycosylated, minimally elaborated compounds **1** and **2** are the least potent. Although the activity of **4** and **6** appears to be anomalous, activity tends to increase with more elaboration of the polyketide-derived backbone. Trisaccharides are more active than disaccharides, which are, in turn, more active than monosaccharides or aglycons. The trisaccharide **15** has a C11-keto group and therefore lacks the furan ring found in **8**. This change results in an almost eight-fold loss of potency; however, the compound still shows significant activity. The O23-phenacylated aglycon **9** and the O23-phenacylated C21a-monosaccharide **7** are equipotent, suggesting that monoglycosylation alone does not confer much potency. Furthermore, a reduction in potency is observed on going from the aglycon **5** to the monoglycoside **6**. A comparison of the potency of **6** and **7** suggests that the presence of the phenacyl group is important for activity. Compounds **8** and **14** differ only by the absence of a C23-*O*-phenacyl group in **14**. This difference results in a 15-fold decrease in the

Table 3. Physicochemical Properties of Elfamycin Antibiotics **1**−**7** and **9**−**15**

	1	**2**	**3**	**4**	**5**	**6**	**7**	**9**	**10**	**11**	**12**	**13**[†]	**14**	**15**
appearance	tan powder	tan powder	tan powder	tan powder	tan powder	tan powder	tan powder	tan powder	tan powder	tan powder	tan powder		tan powder	tan powder
molecular formula	$C_{35}H_{51}NO_9$	$C_{35}H_{51}NO_{10}$	$C_{35}H_{51}NO_{10}$	$C_{36}H_{53}NO_{10}$	$C_{36}H_{53}NO_{11}$	$C_{42}H_{63}NO_{14}$	$C_{50}H_{69}NO_{15}$	$C_{44}H_{59}NO_{11}$	$C_{50}H_{69}NO_{15}$	$C_{50}H_{77}NO_{16}$	$C_{50}H_{77}NO_{16}$	$C_{57}H_{89}NO_{19}$	$C_{57}H_{89}NO_{19}$	$C_{65}H_{95}NO_{21}$
molecular weight	629.4	629.4	645.4	659.4	697.3	805.4	923.5	777.4	923.5	947.5	947.5		1091.6	1225.6
MS (*m/z*)	652.4 (M + Na)[b]	652.4 (M + Na)[b]	646.3 (M + H)[b]	660.4 (M + H)[b]	698.4 (M + Na)[b]	806.5 (M + Na)[b] 828.4 (M + Na)[b]	946.4 (M + Na)[b] 946.4 (M + Na)[b]	800.5 (M + Na)[b]	924.5 (M + Na)[b] 946.4 (M + Na)[b]	970.5 M + Na)[b]	948.5 (M + Na)[b] 970.6 (M + Na)[b]		1114.5 (M + Na)[b]	970.5 (M + Na)[b]
ionization (matrix)	FAB(NBA + NaCl)	FAB(NBA + NaCl)	FAB(NBA)	FAB(NBA)	Electrospray	FAB(NBA)	FAB(NBA + NaCl)	FAB(NBA + NaCl)	FAB(NBA)	FAB(NBA + NaCl)	FAB(NBA)		FAB(NBA + NaCl)	FAB(NBA + NaCl)
solubility: soluble	MeOH, *t*-BuOH, EtOAc	MeOH, *t*-BuOH, EtOAc	MeOH, *t*-BuOH, EtOAc	MeOH, *t*-BuOH, EtOAc	MeOH, *t*-BuOH, EtOAc	MeOH, *t*-BuOH, EtOAc, Me_2CO	MeOH, *t*-BuOH, EtOAc Me_2CO	MeOH, *t*-BuOH, EtOAc, $CHCl_3$	MeOH, *t*-BuOH, EtOAc, Me_2CO	MeOH, *t*-BuOH, EtOAc, Me_2CO	MeOH, *t*-BuOH, EtOAc, Me_2CO		MeOH, *t*-BuOH, EtOAc, Me_2CO	MeOH, *t*-BuOH, EtOAc, $CHCl_3$
insoluble	H_2O, $CHCl_3$	H_2O, $CHCl_3$	H_2O, $CHCl_3$	H_2O, $CHCl_3$	H_2O, $CHCl_3$	H_2O, $CHCl_3$	H_2O, $CHCl_3$	H_2O	H_2O, $CHCl_3$	H_2O, $CHCl_3$	H_2O, $CHCl_3$		H_2O, $CHCl_3$	H_2O
HPLC (t_R, min)[a]	4.5	7.0	6.3	10.3	6.1	5.9	13.2	16.4	15.2	7.0	10.7	8.6	11.6	16.3

[a] Column: B&J ODS 5 (150 × 4.6 mm i.d.); mobile phase: A = 35% CH_3CN−0.1 M NH_4OAc pH 4.0 buffer; B = 75% CH_3CN−0.1 M NH_4OAc pH 4.0 buffer; isocratic for 5 min with 100% A then gradient to 100% B in 15 min.; flow rate: 1.0 mL/min.; detection: Diode array monitored at 297 nm. t_R for **8** = 15.8 min. [b] Compound **13** converted to **14** before physical or spectroscopic data could be acquired.

Table 4. Bioactivity and Bioconversion of Ganefromycin Metabolites

mutant (class)	block	accumulated metabolites	bioactivity[a]	B3M18 (I)	LL2238 (I)	B3M39 (II)	LL2239 (III)	LL2241 (III)	LL4208 (III)
B3M18 (I)	polyketide formation	none							
LL2238 (I)	11 keto reduction/cyclization	**15**	3.1	NC[b]		NC[b]	NC[b]	NC[b]	NC[b]
B3M39 (II)	C23 hydroxylation	**11**, **12**[c]	12.6	**13, 14**	**13, 14**		NC[b]	NC[b]	NC[b]
		13, 14[d]	6.3	NC[b]	NC[b]		NC[b]	NC[b]	NC[b]
LL2239 (III)	C21a-hydroxylation or suger synthesis/attachment	**1, 2**[e]	>100.0	**8**	**8**	consumed[f]		consumed[g]	consumed[g]
		3	100.0	**8**	**8**	**8**		consumed[g]	consumed[g]
		4	6.3	**8**	**8**	**8**		5	consumed[g]
		9	12.5	NC[b]	NC[b]	NC[b]		NC[b]	NC[b]
LL2241 (III)	sugar synthesis/attachment	**5**	50.0	**8**	**8**	**8**	consumed[g]		consumed[g]
LL4208 (III)	C3′-hydroxy methylation or sugar synthesis/attachment	**6**	100.0	**8**	**8**	**8**	**7**[h]	**7**[i]	
		7	12.5	**8**	**8**	**8**	**6**[j]	**10**[k]	
		10	50.0	NC[b]	NC[b]	NC[b]	NC[b]	NC[b]	
LL2057 (wild)		**8**	0.4						

[a] MIC (μg/mL) against *Bacillus megaterium*. [b] NC = Not Converted. [c,d,e] Compounds **11** & **12**; **13** & **14**; and **1** & **2** are epimers. [f] Transformed to epimeric products less polar than starting materials. Some transformation to **11/12** or **13/14** not precluded. [g] Presumed transformed to same metabolites formed in fermentation. [h] Partially converts to **7** and small amount of **10**. [i] Converts to **7** and small amount of **10**. [j] Partially converts to **6** and small amount of **10**. [k] Partially converts to **10**.

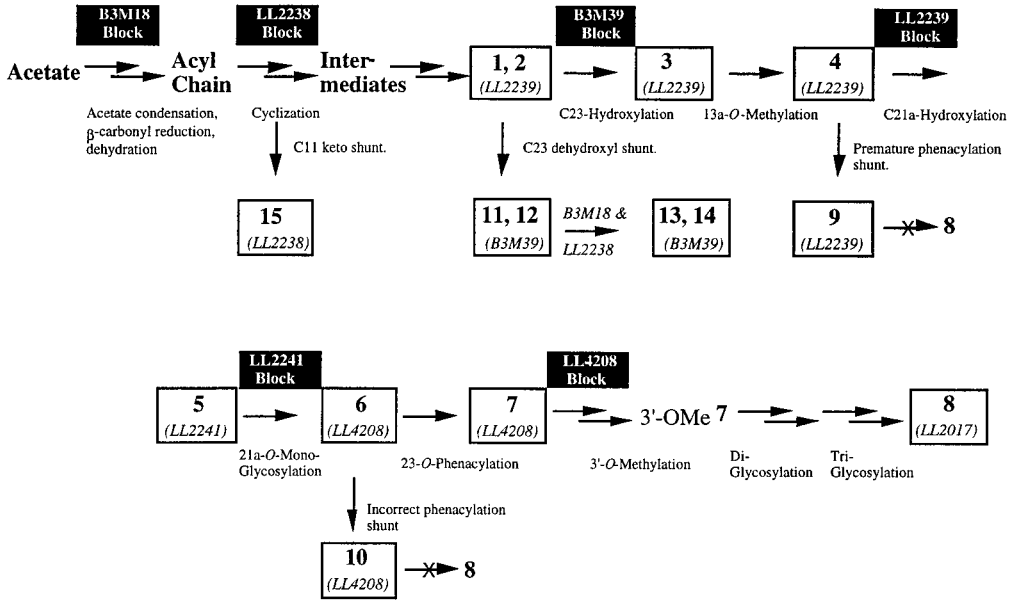

Figure 2. Hypothetical ganefromycin α (***8***) biosynthetic pathway showing relative order of blocked mutants and their products.

potency and also points to the importance of the phenacyl group. Additionally, the activity of the phenacylated C21a-monosaccharides **7** and **10** suggests that the location of the phenacyl group at position 23 enhances potency.

Bioconversion of Ganefromycin Intermediates. Cultures (3 mL) of mutants were fermented for 3 days. Compounds **1**−**7** and **9**−**15** were added to cultures, which were fermented for one or two additional days. Harvested cultures were mixed with an equal volume of MeCN and directly analyzed by HPLC. Retention times, UV spectra, and comparison with pure compounds afforded identification of the bioconverted or unconverted products. Bioconversion results are shown in Table 4. An inspection of the structures produced by the mutants and the ability of the mutants to bioconvert intermediates led to the proposed biosynthetic sequence presented in Figure 2. A number of the isolated metabolites are considered to be true intermediates to ganefromycin, whereas others are presumed shunt metabolites. A fuller discussion of the compounds elaborated by each mutant and the bioconversion behavior that led to the construction of the proposed biosynthetic sequence are presented in the following section.

Mutant Metabolite Profile and Bioconversion Behavior. B3M18, along with 23 similar Class I mutants, produces no observable ganefromycin-type metabolites. Their ability to convert Class III intermediates suggests that they are blocked early in biosynthesis. This is the largest class of mutants, and the mutations are presumed to disrupt the assembly of the polyketide backbone. B3M18 converts all compounds from Class III mutants (except compounds **9** and **10**, which are presumed to be shunt metabolites) to gane-

fromycin α (**8**). This suggests that compounds **1**−**7** are true intermediates in the pathway to **8**.

The inability of B3M18 to bioconvert **9** is most likely a consequence of **9** being a premature phenacylation shunt product and not a true biosynthetic intermediate. B3M18's failure to hydroxylate and further elaborate the C21a position of **9** is possibly due to steric effects caused by the presence of the phenacyl group. This suggests that hydroxylation of C21a normally precedes phenacylation.

B3M18 did not transform compounds **13** and **14** to ganefromycin α. These two compounds are presumed to be shunt metabolites formed in mutant B3M39 (which appears to be blocked in C23-hydroxylation). Though the absence of the hydroxyl group at C23 does not prevent C21a-hydroxylation and subsequent glycosylations, it appears that C23 hydroxylation must occur prior to these events in the biosynthetic sequence. Once the sugars are added, C23 hydroxylation is effectively blocked. Thus, the addition of the third sugar to compounds **11** and **12** is carried out by B3M18 to form **13** and **14**, but no modification occurs at C23.

LL2238 is an atypical Class I mutant that produces **15**, a compound with a keto function at C11 rather than the furan ring formed between C11 and C8. Mutant LL2238 is apparently blocked in the *β*-ketoreductase/cyclase activity directed toward the C-11 keto group. The absence of the furan ring does not preclude completion of the polyketide backbone or further biosynthetic elaboration such that a nonfuran "pseudo-ganefromycin α" (**15**) is formed. It is presumed that the ring closure normally occurs prior to either C23 or C21a hydroxylation, since the earliest isolated intermediates (**1** and **2**) contain the furan ring.

Compound **15** is not bioconverted by any mutant class, which indicates that this fully elaborated, C11-keto molecule does not serve as substrate for ring closure. The MIC of **15** is eight-fold less than **8**, suggesting that the furan ring, which is seen in most members of this class of antibiotics, is important for full bioactivity. This compound does have the best MIC of the metabolites from the mutants, suggesting that a fully elaborated molecule, even without the furan ring, has better MIC value than partially elaborated intermediates. The reduced bioactivity of **15** and the ability of LL2238 to complete all biosynthetic steps other than ring closure would account for its converter classification in cosynthesis experiments.

The leaky Class II B3M39 secretor mutant exhibits a C23-hydroxylation block. This mutant produces minute amounts of ganefromycin α (**8**) along with the C21 epimeric 23-dehydroxy disaccharides and trisaccharides **11**, **12** and **13**, **14**. Although the epimers **11** and **12** are bioconverted by Class I mutants to **13** and **14**, none of these four compounds is converted to ganefromycin α, suggesting that these compounds are shunt products not normally part of the biosynthetic pathway. As discussed previously, a block in C23 hydroxylation does not impede further elaboration at C21a, but once the C21a elaboration occurs, the resulting compounds do not serve as substrates in mutants that are C23 hydroxylation proficient. Thus, C23 hydroxylation normally precedes C21a hydroxylation. This is borne out in the LL2239 metabolites **1**−**4**, which are a collection of metabolites with biosynthetic elaboration at C23 and *O*-methylation at C13a, none of which is hydroxylated at C21a.

B3M39 converts **3**−**7** to ganefromycin α (**8**), while the epimeric **1** and **2** are bioconverted into unknown entities, although in the latter case some bioconversion to the expected **11**−**14** is not precluded. This bioconversion of **3**−**7** would be expected based on the hypothesized block in the biosynthetic sequence.

The Class III mutant LL2239 produces compounds **1**−**4** and **9**, all lacking C21a hydroxylation. Compounds **1** and **2** are epimeric at C21 and lack both C23 hydroxyl and C13a *O*-methyl groups. Compound **3**, while possessing a C23 hydroxyl group, still lacks the C13a *O*-methyl group. Compound **4** is the most elaborated product from this mutant still serving as intermediate in the pathway. It is assumed that the normal biosynthetic sequence proceeds from **1**, **2** through **3** by C23-hydroxylation to **4** via *O*-methylation at C13a (i.e., from least to most elaborated metabolite in the series). Compound **9**, is presumed to appear due to a premature phenacylation of intermediate **4**. The fact that no mutant class bioconverts **9** indicates it to be a shunt metabolite and not a true biosynthetic intermediate.

Compounds **1**−**4** are bioconverted by Class I mutants to ganefromycin α (**8**), as are **3** and **4** by the Class II mutant B3M39, indicating these metabolites to be biosynthetic intermediates. Mutants LL2241 and LL4208, which are blocked later in the biosynthetic sequence, appear to consume **1**−**4**, but do not form **8**. These latter mutants are presumably processing **1**−**4** up to the point of the blocks present in each of these strains (i.e., to compounds **5** and **6**, **7**, **10**, respectively).

The structures accumulated by LL2239 (**1**−**4** and **9**) imply that LL2239 is blocked in C21a hydroxylation, but the mutant appears more complex than that. Its inability to bioconvert **6** or **7** to **8** and **11**,**12** to **13**,**14** suggests a secondary or associated defect in sugar synthesis or attachment(s). Mutant LL2239 does add the phenacyl group to **6** to produce **7**, but the reaction is incomplete and much of the starting **6** remains. Likewise, when **7** is fed to LL2239, **6** is produced. Thus, LL2239 appears to demonstrate that the phenacylation step is readily reversible. It may be that further elaboration (3′-*O*-methylation of the sugar and subsequent glycosylation) may be necessary to move the equilibrium forward, but the secondary defect(s) in LL2239 prevents this. Mutant LL2239's inability to perform sugar attachment is also displayed in it's inability to convert **5** to either **6**, **7**, or **8**. Instead, LL2239 consumes **5**, presumably to **4** (or to the entire series **1**−**4**), in another apparently reversed reaction.

The Class III mutant LL2241 is blocked in the synthesis or addition of sugars to the C21a hydroxyl group. The major product from this mutant is **5**, which is a C21a-hydroxy-**4** and is thus placed later in the biosynthetic sequence. Metabolite **5** is bioconverted to ganefromycin α (**8**) by the Class I mutants and mutant B3M39. As mentioned previously, LL2239 appears to consume **5** to presumably yield its end products **1**−**4**. LL4208 appears to consume **5** in bioconversion, presumably transforming **5** to its accumulated metabolites **6** and **7**.

When compounds **1**−**4** are fed to mutant LL2241 in bioconversion experiments, **1**−**4** are consumed, but no

ganefromycin α (**8**) is produced. These metabolites are presumably converted to **5**, the metabolite normally produced by this mutant. LL2241 doses not transform **11**,**12** to **13**,**14**, which is consistent with an overall defect in sugar synthesis or attachment rather than a specific inability to glycosylate at the C21a hydroxyl group. This last point is borne out by the inability of LL2241 to bioconvert **6** or **7** to **8**. LL2241 retains it's ability to phenacylate in that it partially transforms **6** to **7**.

LL4208 is a leaky Class III secretor mutant that appears to be blocked in the methylation of the 3′-hydroxyl group or addition/synthesis of second and third sugars to the molecule. Mutant LL4208 produces compounds **6**, **7**, **10**, along with traces of **8**. In that compound **6** is less elaborated than **7**, it is considered an earlier intermediate than **7** and is placed as such in the proposed biosynthetic sequence. Similar C13a-*O*-demethyl **6** and **7** structures were observed by Pearce et al.[4] in sinefungin-inhibited fermentations, supporting the notion that the initial glycosylation normally precedes phenacylation. The fact that these C13a-*O*-demethyl-**6** and C13a-*O*-demethyl-**7** structures are observed suggests that C13a-*O*-methylation need not occur prior to C21a hydroxylation and glycosylation. The fact that structures **4**−**7** are C13a-*O*-methylated suggests that this methylation can, and most likely normally does, precede C21a hydroxylation and glycosylation. Also, the fact that **6** and **7** can be converted to **8** indicates that *O*-methylation of the first sugar can occur after attachment to the polyketide backbone.

Metabolite **10** may have resulted from chemical rearrangement and does not appear to be an intermediate in the pathway to **8**, in that none of the mutant strains bioconverted **10**. We have previously demonstrated that a trisaccharide equivalent of **10** (E19020 *β*) is the product of a base-induced 1,2-acyl migration.[8,9] Class I mutants and B3M39 transform **6** and **7** to **8**, confirming them to be biosynthetic intermediates. As mentioned previously, LL2239 and LL2241 phenacylate **6** to yield **7** but do not transform **7** in the forward direction to **8**, consistent with their proposed blocks in sugar formation or attachment.

Mutant LL4208 consumes **1**−**5** but does not produce **8**, presumably converting **1**−**5** to the metabolites normally produced in its fermentation (i.e., **6**, **7**, and **10**). Interestingly, LL4208 does not bioconvert **11**,**12** to **13**,**14**. Thus, even when presented with a transformable substrate with a completed second sugar attached, the third sugar (structurally equal to sugar 1) is not attached. This observation should be considered in light of the metabolites isolated in sinefungin-inhibited fermentations.[4] In that latter case, blocking *O*-methylation of the first sugar did not prevent its attachment but did block subsequent glycosylation. The metabolites from LL4208 are similar, indicating that the first sugar is incompletely synthesized and attached and that its lack of *O*-methylation may be blocking glycosylation with the second sugar. It is likely that **11**,**12** are not glycosylated because the *O*-demethyl sugar 1 or sugar 3 available in LL4208 is not a substrate for this last glycosylation.

Experimental Section

General Experimental Procedures. FABMS were measured on a VG-ZAB SE instrument using the matrixes indicated in Table 3. Electrospray mass spectrum was measured on a VG Quattro triple quadruple mass spectrometer. NMR spectra were recorded on a Bruker AMX 300 spectrometer in deuterated solvents indicated in Tables 1 and 2. A typical NMR data set measured for a compound included carbon, DEPT, proton, COSY, TOCSY (40 ms mixing time), HMQC, and HMBC spectra. In the case of compounds epimeric at C21, NOESY or ROESY spectra were also acquired. All 2D experiments were run nonspinning.

Bacterial Strains and Preservation. Strain LL2057 was used as the starting *S. lydicus* spp. *tanzanius* for mutagensis and subsequent isolation and characterization of blocked mutants. LL2057 is a streptomycin-resistant, improved producer of ganefromycin α originating from a titer improvement program and is derived from *S. lydicus* spp. *tanzanius* NRRL 18036 from a number of mutation/selection cycles. Biological assays employed *B. megaterium* J370. All strains were preserved by adding glycerol to 20% to an overnight culture and storing at −70 °C.

Media and Growth Conditions. *B. megaterium* was grown in 20−10−5 medium (tryptone 20 g L^{-1}, yeast extract 10 g L^{-1}, NaCl 5 g L^{-1}) at 37 °C overnight. Overlays were performed by adding 0.1 mL overnight *B. megaterium* to 4 mL 20−10−5 soft agar (Bacto-agar 0.8 g L^{-1}) and pouring onto the agar dish to be assayed, followed by incubation at 30 °C overnight. *S. lydicus* was grown in Tryptic Soy Broth supplemented with 20 g L^{-1} glucose (TSBG) at 30 °C for 24−48 h. Agar medium for plating, agar production, and cosynthesis was Bennett's agar (NZ-amine A 2 g L^{-1}, yeast extract 1 g L^{-1}, beef extract 1 g L^{-1}, glucose 20 g L^{-1}, Bacto-agar 20 g L^{-1}) incubated at 30 °C for from 3 to 5 days, as required. Fermentation medium M180−15−10M consisted of the following: NZ-amine A 15 g L^{-1}, cornsteep liquor 10 g L^{-1}, maltrin M-180 200 g L^{-1}, glucose 20 g L^{-1}, MES (2-[*N*-morpholino]ethanesulfonic acid) 39 g L^{-1}, $CaCO_3$ 5 g L^{-1}, $(NH_4)_2SO_4$ 2 g L^{-1}, KCl 0.5 g L^{-1}, K_2HPO_4 1 g L^{-1}, $MgSO_4 \cdot 7H_2O$ 0.7 g L^{-1}, $FeSO_4 \cdot 7H_2O$ 0.1 g L^{-1}, $ZnSO_4 \cdot 7H_2O$ 0.05 g L^{-1}, $MnSO_4 \cdot H_2O$ 0.005 g L^{-1}, $CuSO_4 \cdot 5H_2O$ 0.005 g L^{-1}, $CoCl_2 \cdot 6H_2O$ 0.002 g L^{-1}, $NaMoO_4 \cdot 2H_2O$ 0.001 g L^{-1}, and Hodag FD-82 1 mL/L. Fermentations were inoculated from TSBG seeds at 5% and incubated at 30 °C for from 3 to 14 days, as required. Fermentations were conducted in 250-mL Erlenmeyer flasks containing 25 mL of medium at 250 rpm (2″stroke). Bioconversions were conducted in 25-mL Erlenmeyer flasks containing 3 mL of medium.

Mutagenesis. *S. lydicus* strain LL2057 was grown for 24 h in TSBG, sonicated briefly to form fragments from the mycelial tufts, pelleted, and resuspended in fresh TSBG. NTG was added to a final concentration of 20 μg/mL. After incubating at 30 °C for 45 min, the cells were pelleted, washed, and inoculated to TSBG and grown overnight at 30 °C. The resulting mycelial growth was again sonicated briefly, glycerol was added to a final concentration of 20%, and the cells were then aliquoted and frozen at −70 °C.

Isolation and Preliminary Identification of Blocked Mutants. Mutagenized cells were plated onto 500 Bennett's agar plates from a dilution appropriate to achieve ca. 30 colonies per plate. After incubating at

30 °C for 3 days, the plates were overlaid with *B. megaterium* and incubated overnight at 30 °C. The vast majority of the 15 000 colonies tested yielded zones of inhibition of about 6.0−8.0 mm, but 95 colonies that did not produce zones were observed. These latter presumably blocked mutants were streaked to Bennett's agar containing 50 μg/mL streptomycin. Isolated colonies from each presumptive mutant were then stabbed to Bennett's agar, incubated for 3 days, and overlaid. Fifty-six mutants showed no zone or extremely reduced zones in the second round of analysis. These mutants were inoculated to TSBG, and the resulting seeds were used to prepare frozen stock cultures.

Seeds developed from the 56 presumptive mutants were used to grow cells for further agar analysis and preliminary fermentation analysis. The mutants were tested for agar production by swabbing seed culture to Bennett's agar and incubating and overlaying as above. Fermentations were also inoculated and harvested after 7 days of incubation. The mash was diluted 1:5 in MeOH and 10 μL of the filtered extract was analyzed by preliminary low-resolution HPLC. The HPLC system was a 50% MeCN:50% ammonium acetate buffer (0.1 M ammonium acetate, 0.1 M acetic acid) applied in isocratic mode to a C-18 Supelco LC18 column (4.6 × 150 mm, 5 mm dp) with a flow rate of 2 mL/min, monitored at 290 nm. Thirty-two mutants were observed to yield minimal to no zone on agar and no observable ganefromycin α peak by HPLC.

Agar Cosynthesis. The 32 confirmed blocked mutants were analyzed for agar cosynthesis using the method of Delic et al.[12] Converter/secretor interactions were studied by streaking two mutants onto a Bennett's agar plate in two strip patterns of ca. 1.5 in. by 3.75 in., positioned width to width, leaving a region of about 0.3 in. between the mutants. After 3 days of incubation, the plates were overlaid. Zones of inhibition formed at the junction of the two mutants were defined as a complementation reaction. Mutants that displayed a greater portion of the zone of inhibition on their side of the junction were considered to be converters. This analysis allowed the identification of 25 converters, represented by the unique LL2238 and B3M18, which is typical of the remaining 23 of this group. Five strains that acted as strong secretors were identified (LL2239, LL2240, LL2241, LL2243, and LL4208), as well as one weak secretor (B3M39) and a noncomplementing type (LL2237).

Metabolite Identification and Isolation. HPLC of the 7-day fermentation mashes described above revealed that mutants LL2238, B3M39, LL2239, and LL4208 were producing unique ganefromycin-like compounds. Mutant LL2241 was found to be producing an additional novel compound that was also seen in mutants LL2240 and LL2243. All others of the set of 32 mutants showed no evidence of ganefromycin-related metabolites.

Mutants B3M39, LL2238, LL2239, LL2241, and LL4208 were studied throughout a fermentation time course to identify the optimal harvest time for each metabolite and to assess the volume required to allow isolation of sufficient material for structure identification. Mutant LL2238 was fermented for 13 days for isolation of its metabolite, whereas the rest of the mutant set was fermented 4−5 days. From 0.3 L to 3.0 L of mash was generated, as required, by pooling replicate 50-mL fermentations.

Bioconversion. Isolated ganefromycin metabolites were dissolved in MeOH (1 mg/mL) and added to 3-mL fermentations of blocked mutant strains on day 3 at a final concentration of 100 μg/mL. After an additional 1 to 2 days of fermentation, the mashes were harvested and prepared for HPLC analysis by adding an equal volume of CH_3CN, shaking vigorously for 60 s with a vortex mixer, centrifuging, and decanting the supernatant for analysis. The supernatant (20 μL) was analyzed.

HPLC Analysis. HPLC analysis was performed on a HP 1090 liquid chromatograph equipped with a Burdick & Jackson ODS 5 (150 × 4.6 mm i.d.) reversed-phase column. Isocratic elution for 5 min with mobile phase consisting of solvent combination A (35% CH_3CN−0.1 M NH_4OAc buffer adjusted to pH 4.0 with glacial AcOH) was followed by gradient elution to 100% B (75% CH_3CN−0.1 M NH_4OAc pH 4.0 buffer) in 15 min. The flow rate was 1.0 mL/min. Metabolites were detected by monitoring at 297 nm. The retention times of metabolites are shown in Table 3. Isolated compounds were used to confirm peak identities in the chromatograms of mutant extracts.

MIC Determination. Each purified intermediate as well as ganefromycin α was added to 20−10−5 medium to achieve 100 μg/mL. Twofold serial dilutions were then made to a low concentration of 0.098 μg/mL. Exactly 1 mL of each test concentration was inoculated with 0.05 OD_{600} units from a 4-h *B. megaterium* culture. The tubes were incubated at 37 °C overnight. The MIC end-point was defined as the minimum concentration of intermediate that gave an $OD_{600} = 0$.

Compounds 1−4, and 9. After 1750 mL whole mash from LL2239 fermentation was shaken with 875 mL CH_3CN, two layers were observed. After filtration through Celite, the upper CH_3CN layer was removed. The lower aqueous layer was extracted two times with EtOAc. The EtOAc extracts were combined with the CH_3CN layer and evaporated to a small volume that was mostly aqueous. This aqueous sample was filtered through an HP20 column (517 cm^3 bed volume in H_2O) followed by elution with a step gradient from H_2O to CH_3CN in 20% intervals. The HP20 fraction eluting with 60% CH_3CN (583 mg) was chromatographed by HPLC using a Rainin Dynamax 41.4 mm i.d. × 25 cm L C18 column with 35% CH_3CN−65% 0.1 M NH_4OAc pH 4.0 buffer (solvent A) at a flow rate of 40.0 mL/min and detected by UV at 300 nm. After 45 min isocratic elution with solvent A, gradient elution to 100% CH_3CN in 10 min continued to yield **1**, **2**, **3**, and **4** eluting at 21, 38, 35, and 56 min, respectively. The yields of **1**, **2**, **3**, and **4** were 23.0, 31.9, 51.2, and 27.5 mg, respectively, after recovery of the compounds from the mobile phase by extraction with CH_2Cl_2. The fraction eluting from HP20 with 100% CH_3CN (344 mg) was chromatographed by HPLC (Rainin Dynamax 21.4 mm i.d. × 25 cm L C18 column using 70% CH_3CN, 30% 0.1 M NH_4OAc pH 4.0 buffer at a flow rate of 5.0 mL/min and detection by UV at 330 nm) to yield 12.6 mg of **9** eluting after 23.6 min. See Tables 1−3 for spectrocopic and physicochemical data.

Compound 5. Whole mash from mutant LL2241 (300 mL) was shaken with 250 mL CH_3CN and filtered through Celite. H_2O (400 mL) was added to the broth, and the mixture was filtered through column packed with HP20 (bed volume 222 mL) equilibrated with H_2O. After rinsing with 500 mL H_2O, the column was eluted with 400 mL 50% MeOH−H_2O to yield a fraction enriched with **5**. This fraction was chromatographed by HPLC (Rainin Dynamax 41.4 mm i.d. × 25 cm L C18 column; mobile phase 35% CH_3CN−65% 0.1 M NH_4OAc pH 4.0 buffer; flow rate 20.0 mL/min, after 22 min the flow rate was increased to 30 mL/min in 1 min then to 40 mL/min after 40 min in 1 min; detection by UV at 300 nm) to yield **5** eluting after 52 min. Compound **5** (19.3 mg) was recovered from the mobile phase by extraction with EtOAc and appeared as a tan powder after freeze-drying from *t*-BuOH. See Tables 1−3 for spectrocopic and physicochemical data.

Compounds 6, 7, and 10. When 1650 mL whole mash from LL4208 fermentation was shaken with 825 mL CH_3CN, two layers were observed. After filtration through Celite, the upper CH_3CN layer was removed. The lower aqueous layer was extracted two times with EtOAc. The EtOAc extracts were recovered, combined with the CH_3CN layer, and evaporated to a small volume. Filtration through HP20 (517 cm^3 bed volume) and subsequent step-gradient elution yielded fractions eluting with 60% and 80% CH_3CN−H_2O. The HP20 fraction eluting with 60% CH_3CN (616 mg) was chromatographed by HPLC using a Rainin Dynamax 41.4 mm i.d. × 25 cm L C18 column with 50% CH_3CN−50% 0.1 M NH_4OAc pH 4.0 buffer at a flow rate of 20.0 mL/min and detected by UV at 330 nm to yield compound **6** (188 mg) eluting after 39 min. The HP20 fraction eluting with 80% CH_3CN−H_2O (831 mg) was chromatographed by HPLC (Rainin Dynamax 41.4 mm i.d. × 25 cm L C18 column using 45% CH_3CN, 55% 0.1 M NH_4OAc pH 4.0 buffer at a flow rate of 40 mL/min and detection by UV at 254 nm) to yield 193 mg of **7** eluting after 30 min and 91 mg of **10** eluting after 63 min. Compounds **6**, **7**, and **10** were recovered from the mobile phase by extraction into EtOAc, evaporation of solvent, and freeze-drying from *t*-BuOH. See Tables 1−3 for spectrocopic and physicochemical data.

Compounds 11−14. The whole mash (2200 mL) from mutant B3M39 was shaken with 1800 mL CH_3CN and filtered through Celite. After evaporation of most of the CH_3CN, the filtrate was put through an HP20 column (517 cm^3 bed volume) followed by rinsing with 2 L of H_2O and step-gradient elution with solvent combinations starting from 50% CH_3CN−H_2O in 10% increments. A portion of the HP20 fraction eluting with 60% CH_3CN−H_2O was chromatographed by HPLC (Rainin Dynamax 41.4 mm i.d. × 25 cm L C18 column using 35% CH_3CN−65% 0.1 M NH_4OAc pH 4.0 buffer at a flow rate of 20 mL/min and detection by UV at 300 nm; flow was increased to 30 mL/min after 34 min) to yield 47 mg of **11** and 20 mg of **13** eluting after 66 and 80 min, respectively. The HPLC column was washed with 50% CH_3CN−50% buffer to yield a fraction enriched in compounds **12** and **14**. Approximately 6% of this enriched fraction was rechromatographed on HPLC (Rainin Dynamax 21.4 mm i.d. × 25 cm L C18 column using 40% CH_3CN−60% 0.1 M NH_4OAc pH 4.0 buffer at a flow rate of 9.9 mL/min and detection by UV at 330 nm) to yield 6.1 mg of **12** and 1.6 mg of **14** eluting after 45 and 55 min, respectively. Compounds **11** and **13** epimerized to form compounds **12** and **14**, respectively, upon standing in Me_2CO or MeOH solutions at 25 °C. See Tables 1−3 for spectrocopic and physicochemical data.

Compound 15. Freeze-dried whole mash (28 g) from a 300-mL fermentation of LL2238 was extracted with MeOH to yield 6.5 g of a brown, oily crude extract, which was chromatographed on C18 via VLC (41.5 cm^3 bed volume of 8 μm; 60 Å Dynamax C18) using a step gradient to give a 762-mg fraction eluting with 80% MeOH−H_2O. HPLC chromatography (Rainin Dynamax 21.4 mm i.d. × 25 cm L C18 column using 70% CH_3CN−30% 0.1 M NH_4OAc pH 4.0 buffer at a flow rate of 5.0 mL/min and detection by UV at 260 nm) of this fraction yielded 29 mg of **15** eluting after 15 min. Compound **15** was recovered from the mobile phase by extraction with EtOAc. See Tables 1−3 for spectrocopic and physicochemical data.

Acknowledgment. The authors wish to thank B. Hancock, N. Strathy, and R. Szuch for their very capable technical assistance. We are indebted to Dr. R. Tsao for measuring the FABMS data. We thank Dr. K. Janota for measuring the electrospray MS data. We acknowledge Drs. M. Tischler, G. Schlingmann, and F. Koehn for helpful and insightful discussions. Drs. A. Sutherland and D. Abbanat are acknowledged for providing critical and constructive feedback about the manuscript.

References and Notes

(1) Carter, G. T.; Phillipson, D. W.; Goodman, J. J.; Dunne, T. S.; Borders, D. B. *J. Antibiotics* **1988**, *41*, 1511−1514.
(2) Maiese, W. M.; Lechevalier, M. P.; Lechevalier, H. A.; Korshalla, J.; Goodman, J.; Wildey, M. J.; Kuck, N.; Conner, S. D.; Greenstein, M. *J. Antibiot.* **1989**, *42*, 1489−1493.
(3) West, R. R.; Carter, G. T.; Pearce, C. J.; Borders, D. B. In *International Research Congress on Natural Products. 32nd Annual Meeting of the American Society of Pharmacognosy*; Chicago, IL, 1991; p 110.
(4) Pearce, C. J.; West, R. R.; Carter, G. T. *Tetrahedron Lett.* **1995**, *36*, 1809−1812.
(5) Liu, C.-M.; Maehr, H.; Leach, M.; Liu, M.; Miller, P. A. *J. Antibiot.* **1977**, *30*, 416−419.
(6) Liu, C.-M.; Williams, T. H.; Pitcher, R. G. *J. Antibiot.* **1979**, *32*, 414−417.
(7) Nielsen, J. B. K. *J. Cell. Biochem. Suppl.* **1990**, *14A*, 119 (abstract).
(8) Carter, G. T.; Phillipson, D. W.; West, R. R.; Borders, D. B. *J. Org. Chem.* **1993**, *58*, 6588−6595.
(9) Carter, G. T.; Tischler, M.; West, R. R.; Bailey, A. E. J. *Antibiot.* **1995**, *48*, 1312−1319.
(10) McDonald, L. A.; Lotvin, J. A.; Bailey, A. T.; Carter, G. T. In *Thirty-Sixth Annual Meeting of the American Society of Pharmacognosy*; Oxford, MS, 1995; Abstract P-162.
(11) Delic, V.; Hopwood, D. A.; Friend, E. *J. Mutation Res.* **1970**, *9*, 167−182.
(12) Delic, V.; Pigac, J.; Sermonti, G. *J. Gen. Microbiol.* **1969**, *55*, 103−108.

NP970408I